VELIVOLI - Profili e spessori percentuali

MONOMOTORE AD ELICA	corda alla radice [m]	profilo o spessore perc alla radice	profilo o spess perc all'estremità
Cessna Skyhawk		NACA 2412	NACA 2412
Cessna Skylane		2412	2412
Cessna Centurion		64A215	64A412
Cessna Crusader		23017	23012
Beechcraft		23016	23012
Piper Warrior		65-415	
BIMOTORI AD ELICA			
Beechcraft Kingair		23018	23011
Cessna Crusader		23017	23012
Cessna 402C		23018	23009
Piper Mojave		63-415	63-212
P68		63-3-515	63-3-515
TURBOELICA TRASP REG.			
ATR42		18%	13%
Fokker 50		64-421	64-415
VELIVOLI DA TRASP A GETTO			
DC10	10.71	12.2%	8.4%
A300	8÷9	10.5%	
B747	16.56	13.4%	8%
Fokker 100	5.3	12.3%	9.6%

2

Table A6.1 *Low-speed aerofoil section aerodynamic properties – NACA experimental data from Abbott and Von Doenhoff [44]*

Aerofoil	α_0 (deg)	C_{M_0}	a_{lrad}	$C_{l_{\alpha/\text{deg}}}$	$\alpha_{C_{L\max}}$ (deg)	$C_{L\max}$	Section Cd at $C_{L\max}$
0006	0	0	6.19	0.108	9.0	0.92	0.0095
0009	0	0	6.25	0.109	13.4	1.32	0.0124
23012	−1.4	−0.014	6.13	0.107	18.0	1.79	0.016
23015	−1.0	−0.007	6.13	0.107	18.0	1.72	0.02
23018	−1.2	−0.005	5.96	0.104	16.0	1.60	0.016
23021	−1.2	0	5.90	0.103	15.0	1.50	0.0162
63–006	0	0.005	6.42	0.112	10.0	0.87	0.0086
63–009	0	0	6.36	0.111	11.0	1.15	0.0113
63–206	−1.9	−0.037	6.42	0.112	10.5	1.06	0.008
63–209	−1.4	−0.032	6.30	0.11	12.0	1.4	0.0127
63–210	−1.2	−0.035	6.47	0.113	14.5	1.56	0.014
63_1–012	0	0	6.65	0.116	14.0	1.45	0.0134
63_1–212	−2.0	−0.035	6.53	0.114	14.5	1.63	0.0117
63_1–412	−2.8	−0.075	6.70	0.117	15.0	1.77	0.0154
63A 010	0	0.005	6.02	0.105	13.0	1.2	0.0146
63A 210	−1.5	−0.04	5.9	0.103	14.0	1.43	0.014
64–006	0	0	6.25	0.109	9.0	0.8	0.007
64–009	0	0	6.3	0.11	11.0	1.17	0.0126
64–206	−1.0	−0.04	6.3	0.11	12.0	1.03	0.009
64–210	−1.6	−0.04	6.3	0.11	14.0	1.45	0.0118
64_1–412	−2.6	−0.065	6.42	0.112	15.0	1.67	–
64A 010	0	0	6.3	0.11	12.0	1.23	0.011
64A 210	−1.5	−0.04	6.02	0.105	13.0	1.44	0.011
64A 410	−3.0	−0.08	5.73	0.10	15.0	1.61	0.012
64_1A 212	−2.0	−0.04	5.73	0.10	14.0	1.54	0.012
64_2A 215	−2.0	−0.04	5.44	0.095	15.0	1.5	0.016
65–006	0	0	6.02	0.105	12.0	0.92	0.008
65–009	0	0	6.13	0.107	11.0	1.08	0.012
65–206	−1.6	−0.031	6.02	0.105	12.0	1.03	0.009
65–210	−1.6	−0.034	6.19	0.108	13.0	1.4	0.0137

$R_e = 9 \times 10^6$, smooth leading-edge.

The first integer indicates the maximum value of the mean-line ordinate y_c in per cent of the chord. The second integer indicates the distance from the leading edge to the location of the maximum camber in tenths of the chord. The last two integers indicate the section thickness in per cent of the chord. Thus the NACA 2415 wing section has 2% camber at 0.4 of the chord from the leading edge and is 15% thick.

Table A6.2 *Section aerodynamic properties – advanced aerofoil sections at high subsonic speeds*

Aerofoil	C_L	C_{M_0} at cruise	a_1/rad	$C_{L\alpha}$/deg	$c_{L_{max}}$ (Low speed)	Section Cd at given cruise C_L at M_D	t/c max	M drag rise at given C_L	Reference for data
RAE9515	0.3	−0.106	6.47	0.163	1.0	0.013	0.105	0.79	RAE R&M 3820, 1978 [45]
	0.4	−0.106	(Low Speed)			0.013		0.79	
	0.5	−0.11				0.013		0.79	
	0.6	−0.12				0.014		0.79	
RAE9530	0.3	−0.12	5.84	0.102	1.23	–	0.105	0.80	RAE R&M 3820, 1978 [45]
	0.4	−0.12	(Low Speed)			0.015		0.795	
	0.5	−0.13				0.015		0.79	
	0.6	−0.5				0.018		0.78	
RAE9550	0.3	−0.08	6.88	0.12	1.08		0.122	0.775	RAE R&M 3820, 1978 [45]
	0.4	−0.09						0.77	
	0.5	−0.095						0.765	
	0.6	−0.01						0.72	
RAE5225	0.3	−0.08			–	0.0107	0.14	–	RAE TR 87002 [46]
	0.4	−0.10			all at	0.0107		–	
	0.5	−0.1			M = 0.735	0.011		–	–
RAE5230	0.6	−0.1				0.0114		0.735	RAE TR87002 [46]
	0.3	−0.1				0.0112	0.14	–	–
	0.4	−0.1			all at	0.0111		–	
	0.5	−0.1			M = 0.735	0.011[illegible]			–
RAE5236	0.5	−0.1				0.012		0.735	RAE TR87002 [46]
	0.3	−0.076				0.0111	0.14		–
	0.4	−0.078			all at	0.0113			–
	0.5	−0.076			M = 0.735	0.0116			
	0.6	−0.076				0.0122		0.735*	
NACA SC(3)	0.3	−0.17			all at	0.0122	0.12		NASA TM−86371 [47]
−0712(B)	0.4	−0.18			M = 0.78	0.014			–
	0.5	−0.18			$R_e = 30 \times 10^6$	0.018			–
	0.6	−0.18				0.021		0.80**	
DSMA523	0.3	–			all at	0.012	0.11		NASA TM−81336 [48]
	0.4	–			M = 0.8	0.012			
	0.5	–			$R_e = 14.5 \times 10^6$	0.013			
	0.6	–				0.016		0.8	

* At $C_L = 0.58$ ** at $C_L = 0.68$.

Table 6.1 Homebuilt Airplanes: Wing Geometric Data

Type	Dihedral Angle, Γ_w, deg.	Incidence Angle, i_w, root/tip deg.	Aspect Ratio, A	Sweep Angle, $\Lambda_{c/4}$, deg.	Taper Ratio, λ_w	Max. Speed, V_{max}, kts	Wing Type
PIK-21 Durable	0	0	3.8	0	1.0	NA	ctl/low
RD-03C PIEL	6.5	3/0	7.0	0	0.51	182	ctl/mid
CP-750	5.7	4.2	5.9	0	0.55	183	ctl/low
CP-90 POTTIER	5.7	3	5.4	0	0.44	171	ctl/low
P-50R	4.4	NA	5.1	2	0.54	167	ctl/low
P-70S O-O	0	2	4.8	0	1.0	129	ctl/mid
Aerosport Aerocar	2.5	NA	5.7	0	1.0	76	ctl/low
Micro-Imp Coats	0	4	4.7	0	1.0	260	ctl/high
SA-III Sequoia	4	1.5	5.6	0	1.0	165	ctl/low
300 Ord-Hume	3	3.5/1.5	6.9	0	0.55	243	ctl/low
OH-4B Procter	3	3	5	5.0	1.0	95	brcd/parasol
Petrel	5	0	6.6	0	1.0	113	ctl/low
Bede BD-8	0	3	3.9	0	1.0	238	ctl/low

ctl = cantilever brcd = braced (strutted)

Table 6.2 Single Engine Propeller Driven Airplanes: Wing Geometric Data

Type	Dihedral Angle, Γ_w, deg.	Incidence Angle, i_w, root/tip deg.	Aspect Ratio, A	Sweep Angle, $\Lambda_{c/4}$, deg.	Taper Ratio, λ_w	Max. Speed, V_{max}, kts	Wing Type
CESSNA							
Skywagon 207	1.7	1.5/-1.5	7.4	0	0.69	182	brcd/high
Cardinal RG	1.5	4.1/0.7	7.3	0	0.73	156	ctl/high
Skylane RG	1.7	0.8/-2.8	7.4	0	0.67	187	brcd/high
PIPER							
Cherokee Lance	7.0	2/-1	6.2	0	1.0	188	ctl/low
Cher. Warrior	7.0	2/-1	7.2	5	0.67	152	ctl/low
Turbo Sarat.SP	6.8	NA	7.3	0	0.68	195	ctl/low
Bellanca Skyrocket	2	.2	6.7	0	0.57	287	ctl/low
Grumman Am. Tiger	5	1.4	7.1	0	1.0	148	ctl/low
Rockwell Commander 112A	7	2	7.0	-2.5	0.50	180	ctl/low
Trago Mills SAH-1	5	3/1	7.5	0	0.54	202	ctl/low
Scottish Aviation Bullfinch	6.5	1.2	8.4	0	0.57	150	ctl/low
Robin HR100/4	6.3	4.7	5.4	0	1.0	180	ctl/low
Socata Rallye 235E	7	4	7.6	0	1.0	148	ctl/low
Fuji FA-200	7	2.5	6.3	0	1.0	123	ctl/low
Gen Avia F15F	6	4	7.7	0	0.49	167	ctl/low

ctl = cantilever brcd = braced (strutted)

Table 6.3 Twin Engine Propeller Driven Airplanes: Wing Geometric Data

Type	Dihedral Angle, Γ_w, deg.	Incidence Angle, i_w, root/tip deg.	Aspect Ratio, A	Sweep Angle, $\Lambda_{c/4}$, deg.	Taper Ratio, λ_w	Max. Speed, V_{max}, kts	Wing Type
CESSNA							
310R	5	2.5/-.5	7.3	0	0.67	236	ctl/low
402B	5 (outer)	2/-.5	7.5	0 L.E.	0.67	227	ctl/low
414A	5	2.5/-.5	8.6	0 L.E.	0.60	232	ctl/low
T303	7	3/0	8.1	0 L.E.	0.71	216	ctl/low
PIPER							
PA-31P	6	1/-1.5	7.2	0	0.39	243	ctl/low
PA-44-180T	7.2	NA	8.1	0	0.63	196	ctl/low
Chieftain	5	1/-1.5	7.2	1.9	0.40	231	ctl/low
Cheyenne I	5	1.5/-1	7.4	0	0.37	249	ctl/low
Cheyenne III	5	1.5	7.8	0	0.31	296	ctl/low
BEECH							
Duchess 76	6.5	3/.6	8.0	0	0.80	194	ctl/low
Duke B60	6	4/0	7.2	0	0.32	246	ctl/low
Learfan 2100	4	1.5	9.5	0	0.45	369	ctl/low
Rockwell Commander 700	7	NA	9.0	0	0.43	231	ctl/low
Piaggio P166-DL3	21.5/2.5*	2.7	7.3	7.5	0.35	215	ctl/gull
EMB-121	7	3	7.2	0.33	0.61	316	ctl/low

ctl = cantilever brcd = braced (strutted)
*21.5 inboard, 2.5 outboard on this gull wing configuration

Table 6.4 Agricultural Airplanes: Wing Geometric Data

Type	Dihedral Angle, Γ_w, deg.	Incidence Angle, i_w, root/tip deg.	Aspect Ratio, A	Sweep Angle, $\Lambda_{c/4}$, deg.	Taper Ratio, λ_w	Max. Speed, V_{max}, kts	Wing Type
IAR-822	5 (outer)	5	6.3	0	1.0	92	ctl/low
UTVA-65	2	2.5	7.2	0	0.7	95	brcd/low
IA-53	7.5 (out)	4.3	6.3	0	0.7	116	ctl/low
EMB-200	7	3	7.0	0	1.0	116	ctl/low
Ag-cat	3	6	8.7	0	1.0	113	brcd/bipl
WSK M-15	NA	NA	NA	0	NA	146	brcd/bipl
PZL M-18A	1.3	3	7.8	0	1.0	128 138*	ctl/low
PZL 106A	4	6.5	7.8	4	1.0	114*	brcd/low
NDN-6	4.3	4.5	7.5	0	0.7	135	brcd/low
Cessna AgBusky	9	1.5/-1.5	8.5	0	0.7	106	brcd/low
Antonov AN-2M	2.5 both wings	NA	NA	0	1.0	136	brcd/bipl
HAL-31	6	0	6.0	0	1.0	108	ctl/low

*speed without spray equipment installed
ctl = cantilever brcd = braced (strutted) bipl = biplane

Table 6.5 Business Jets: Wing Geometric Data

Type	Dihedral Angle, Γ_w, deg.	Incidence Angle, i_w, root/tip deg.	Aspect Ratio, A	Sweep Angle, $\Lambda_{c/4}$, deg.	Taper Ratio, λ_w	Max. Speed, V_{max}, kts	Wing Type
DASSAULT/BREGUET							
Falcon 10	1.5	NA	7.1	27	0.36	492(25K)	ctl/low
Falcon 20F	2	1.5	6.4	30	0.31	465(25K)	ctl/low
Falcon 50	0	NA	7.6	24	0.32	475	ctl/low
CESSNA							
Citation I 500	4	2.5/-0.5	7.8	0	0.39	277(28K)	ctl/low
Citation II	4.7	NA	8.3	2	0.32	277(28K)	ctl/low
Citation III	2.8	NA	8.9	25	0.35	472(33K)	ctl/low
GATES LEARJET							
24	2.5	1	5.0	13	0.50	473(31K)	ctl/low
35A	2.5	1	5.7	13	0.50	464	ctl/low
55	2.9	NA	7.3	13	0.42	470(30K)	ctl/low
IAI							
1124 Westw. I	2	1/-1	6.5	5	0.33	471	ctl/mid
1125 Astra	2.6 (out)	NA	8.8	34/25 at LE	0.30	472(35K)	ctl/low
Canadair CL601	2.3	3	8.5	25	0.26	450	ctl/low
BAe 125-700	2	2.1/-0.3	6.3	20	0.28	436(28K)	ctl/low
GA Gulfst. III	3	3.5/-0.5	6.5	28	0.31	487	ctl/low
Mu Diamond I	2.7	3/-3.5	7.5	20	0.35	431(30K)	ctl/low
L. Jetstar II	2	1/-1	5.3	30	0.37	475(30K)	ctl/low

ctl = cantilever (30K) = 30,000 ft altitude

Table 6.6 Regional Turbopropeller Driven Airplanes: Wing Geometric Data

Type	Dihedral Angle, Γ_w, deg.	Incidence Angle, i_w, root/tip deg.	Aspect Ratio, A	Sweep Angle, $\Lambda_{c/4}$, deg.	Taper Ratio, λ_w	Max. Speed, V_{max}, kts	Wing Type
CASA C-212-200							
SHORTS							
330	3 (outer)	NA	12.3	0	1.0	190(10K)	brcd/high
360							
BEECH							
1900	6	3.5/-1.1	9.8	0	0.42	263(8K)	ctl/low
B99	7	4.8	7.5	0	0.5	247(12K)	ctl/low
CESSNA CONQUEST							
I							
II							
GA Gulfstr. Ic							
GAF N22B							
Fokker F27-200	2.5	3.5	12.0	0	0.41	259(20K)	ctl/high
DeHAVILLAND CANADA							
DHC-6-300							
DHC-7	4.5	3	10.0	0	0.44	231(8K)	ctl/high
DHC-8	2.5 (out)	NA	12.3	0	0.45	270(15K)	ctl/high
EMB 110	7	3	9.9	0	0.50	248(8K))	ctl/low
EMB 120	6.5	2	9.9	0	0.50	NA	ctl/low
BRITISH AEROSPACE							
Jetstream 31	7	2	10.0	0.5	0.37	263(20K)	ctl/low
748	7	3	12.7	2.9	0.36	244(15K)	ctl/low

ctl = cantilever (30K) = 30,000 ft altitude

Table 6.7 Jet Transports: Wing Geometric Data

Type	Dihedral Angle, Γ_w, deg.	Incidence Angle, i_w, root/tip deg.	Aspect Ratio, A	Sweep Angle, $\Lambda_{c/4}$, deg.	Taper Ratio, λ_w	Max. Speed, V_{max}, kts	Wing Type
BOEING							
727-200	3	2	7.1	32	0.30	549(22K)	ctl/low
737-200	6	1	8.8	25	0.34	462(33K)	ctl/low
737-300	6	1	8.0	25	0.28	462(33K)	ctl/low
747-200B	7	2	7.0	37.5	0.25	523(30K)	ctl/low
747SP	7	2	7.0	37.5	0.25	529(30K)	ctl/low
757-200	5	3.2	7.9	25	0.26		ctl/low
767-200	6	4.3	7.9	31.5	0.27		ctl/low
McDONNELL DOUGLAS							
DC-9 Super 80	3	1.3	9.6	24.5	0.16	500	ctl/low
DC-9-50	1.5	NA	8.7	24	0.18	537	ctl/low
DC-10-30	5.3/3	+/-	7.5	35	0.25	530(25K)	ctl/low
AIRBUS							
A300-B4	5	NA	7.7	28	0.35	492(25K)	ctl/low
A310	11.1/4.1	5.3	8.8	28	0.26	483(30K)	ctl/low
Lockh.1011-500	7.5/5.5	NA	7.0	35	0.30	525(30K)	ctl/low
Fkr F28-4000	2.5	NA	8.0	16	0.31	390	ctl/low
Rombac 111-495	2	2.5	8.5	20	0.32	470(21K)	ctl/low
BAe 146-200	-3	3.1/0	9.0	15	0.36	420(26K)	ctl/high
Tupolev Tu154	0	NA	7.0	35	0.27	526(31K)	ctl/low

ctl = cantilever (30K) = 30,000 ft altitude

Table 6.8 Military Trainers: Wing Geometric Data

Type	Dihedral Angle, Γ_w, deg.	Incidence Angle, i_w, root/tip deg.	Aspect Ratio, A	Sweep Angle, $\Lambda_{c/4}$, deg.	Taper Ratio, λ_w	Max. Speed, V_{max}, kts	Wing Type
Propeller Driven							
EMB-312 Tucano	5.5	1.4/-0.8	6.4	0.7	0.47	292	ctl/low
Pilatus PC-7	7 (outer)	NA	6.5	1	0.55	270	ctl/low
NDN-1	5 (outer)	3	5.4	0	0.79	247	ctl/low
Beech T-34C	7	4/1	6.2	0	0.41	280	ctl/low
Aerosp.Epsilon	5	2	7.0	0	0.63	281	ctl/low
SM SF-260M	6.3	2.8/0	6.3	0	0.49	235	ctl/low
Yak-52	2	2	5.8	0	0.54	194	ctl/low
Neiva T-25	6	2	7.1	0	0.54	269	ctl/low
Jet Driven							
Aero L-39C	2.5	2	4.4	2	0.52	491	ctl/low
Microjet 200B	5	3	8	0	0.39	300	ctl/low
DB/D Alphajet	-6	NA	4.8	28	0.36	495(33K)	ctl/shldr
Aermac. MB339A	2.6	NA	5.3	9	0.58	500	ctl/low
SM S-211	-2	2.2/-1.3	5.1	16	0.46	400	ctl/shldr
PZL TS-11	2.7	NA	5.7	7	0.51	404	ctl/mid
CASA C-1-1	5	1	5.6	2	0.60	428(25K)	ctl/low
Bae Hawk Mk1	2	NA	5.3	22	0.34	572	ctl/low
Tupolev Tu154	0	NA	7.0	35	0.27	526(31K)	ctl/low

ctl = cantilever shldr = shoulder (30K) = 30,000 ft altitude

8.

Table 6.9 Fighters: Wing Geometric Data

Type	Dihedral Angle, Γ_w, deg.	Incidence Angle, i_w, root/tip deg.	Aspect Ratio, A	Sweep Angle, $\Lambda_{c/4}$, deg.	Taper Ratio, λ_w	Max. Speed, V_{max}, kts	Wing Type
DASSAULT BREGUET							
Mirage III-E	-1	0	1.9	61(LE)	0	1,268(39K)	ctl/low
Mirage F1-C	-4.5	NA	2.8	48(LE)	0.29	1,260	ctl/shldr
Mirage 2000	-1	NA	2.0	58(LE)	0	1,260	ctl/low
Super Etendard	-3.5	NA	3.2	45	0.50	573	ctl/mid
Fairch.R.A-10A	7 (outer)	-1	6.5	0	0.66	450	ctl/low
Grumman A-6E	0	NA	5.3	25	0.30	700	ctl/mid
Grumman F14A	-1.5(out)	NA	7.3*	20/68(LE)	0.40	M = 2.4	vsw/high
Northrop F-5E	0	0	3.8	24	0.19	710	ctl/low
Vought A-7E	-5	-1	4	35	0.25	595(5K)	ctl/high
McDONNELL DOUGLAS							
F-4E	0/12	NA	2.8	45(LE)	0.18	1,146	ctl/low
F-15	-1	0	3.0	39	0.25	M =2.5	ctl/high
AV-8B	-12	1.8	4.0	24	0.28	585(0K)	ctl/shldr
GD FB-111A	0	NA	7.6*	16/73(LE)	0.33	1,260	ctl/shldr
GD F-16	0	0	3.0	40(LE)	0.22	495(33K)	ctl/mid
Cessna A37B	3	3.6/1	6.2	0	0.68	455	ctl/low
Aerm. MB339K	2.6	NA	5.3	8.5	0.58	500	ctl/low
Sukhoi Su-7BMK	0	NA	2.6	62(LE)	0.26	730(0K)	ctl/mid

ctl = cantilever   shldr = shoulder   (30K) = 30,000 ft altitude
* taken at lowest sweep angle

Table 6.10 Military Patrol, Bomb and Transport Airplanes: Wing Geometric Data

Type	Dihedral Angle, Γ_w, deg.	Incidence Angle, i_w, root/tip deg.	Aspect Ratio, A	Sweep Angle, $\Lambda_{c/4}$, deg.	Taper Ratio, λ_w	Max. Speed, V_{max}, kts	Wing Type
Turbopropeller Driven							
Lockh'd C130E	2.5	3/0	10.1	0	0.49	325	ctl/high
Lockheed P3C	6	0/0.5	7.5	0	0.40	411(15K)	ctl/low
Antonov 12BP	-3.8(out)	NA	11.9	7.4	0.34	419	ctl/high
Antonov 22	-3.5	NA	12.0	3	0.36	399	ctl/high
Antonov 26	-2(out)	3	11.7	7	0.34	NA	ctl/high
Grumman E2C	3.1	NA	9.3	5.3	0.34	325	ctl/high
DB Atlantic 2	6 (outer)	3	11.6	9 (LE)	0.39	348	ctl/low
Aerital.G222	2.5 (out)	NA	9.2	2.1	0.50	291	ctl/high
Transall C-160	3.5 (out)	NA	10.0	1.9	0.50	320	ctl/high
Jet Driven							
Lockheed S3A	0	3/-3.5	7.9	15	0.25	450	ctl/high
Lockh'd C-141B	-3.5	NA	7.5	25.5	0.41	492	ctl/high
Lockheed C-5A	-5.1	NA	7.8	25.6	0.34	496(25K)	ctl/high
BAe Nimrod Mk2	2.7	NA	6.2	20	0.23	500	ctl/low
Boeing YC-14	0	NA	9.4	4.6	0.30	438	ctl/high
McDD KC-10A	5/3	+/-	7.5	35	0.25	530(25K)	ctl/low
Tupolev Tu-16	-3.7	NA	6.6	43(LE)	0.44	535(6K)	ctl/high
Tupolev Tu-22	0	NA	4.0	51(LE)	0.31	800(40K)	ctl/mid
Ilyushin Il76T	-3.6	NA	11.7	25	0.37	459	ctl/high

ctl = cantilever   shldr = shoulder   (30K) = 30,000 ft altitude

Although the possibility of such airfoils was known for some time, their successful development in modern times is attributed to R. T. Whitcomb. A Whitcomb-type supercritical airfoil is pictured in Figure 3.7.

Tested at low speeds, the supercritical airfoils were found to have good $C_{l_{max}}$ values as well as low C_d values at moderate lift coefficients. As a result, another family of airfoils evolved from the supercritical airfoils, but for low-speed applications. These are the "general aviation" airfoils, designated GA(W) for general aviation (Whitcomb). The GA(W)-1 airfoil is the last of the

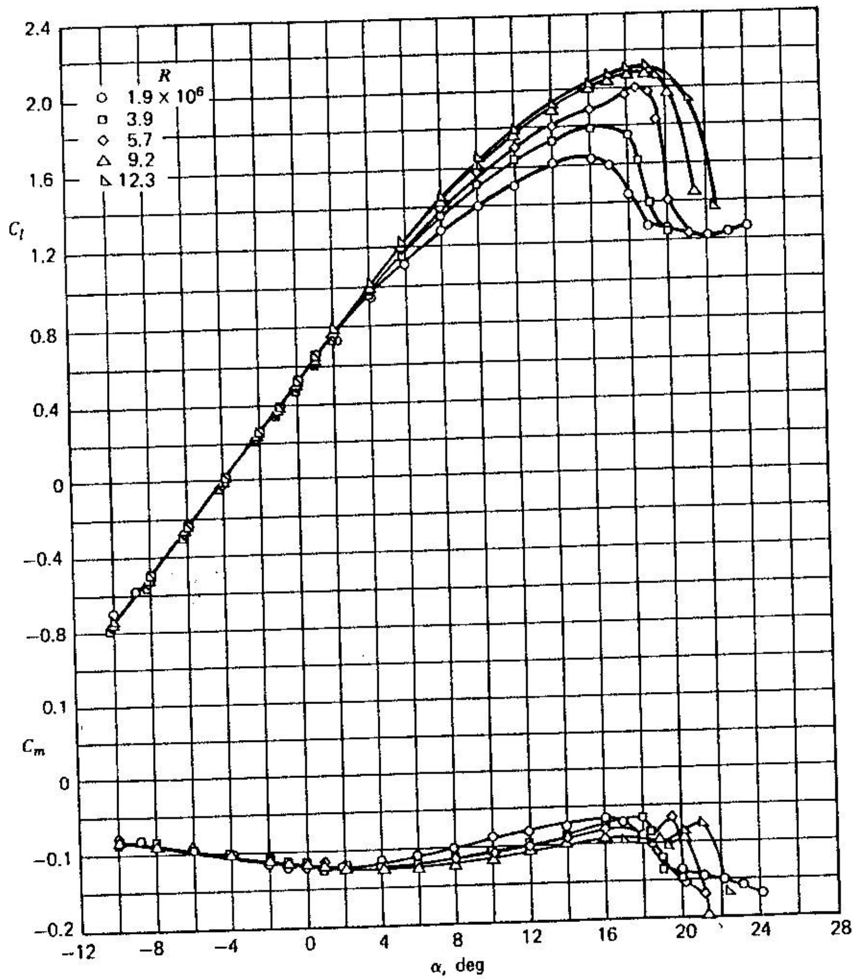

Figure 3.10a Effect of Reynolds number on section characteristics of the

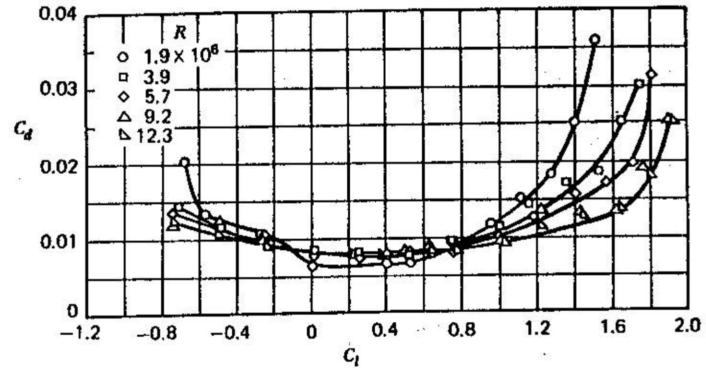

Figure 3.10b Conditions same as Figure 3.10a.

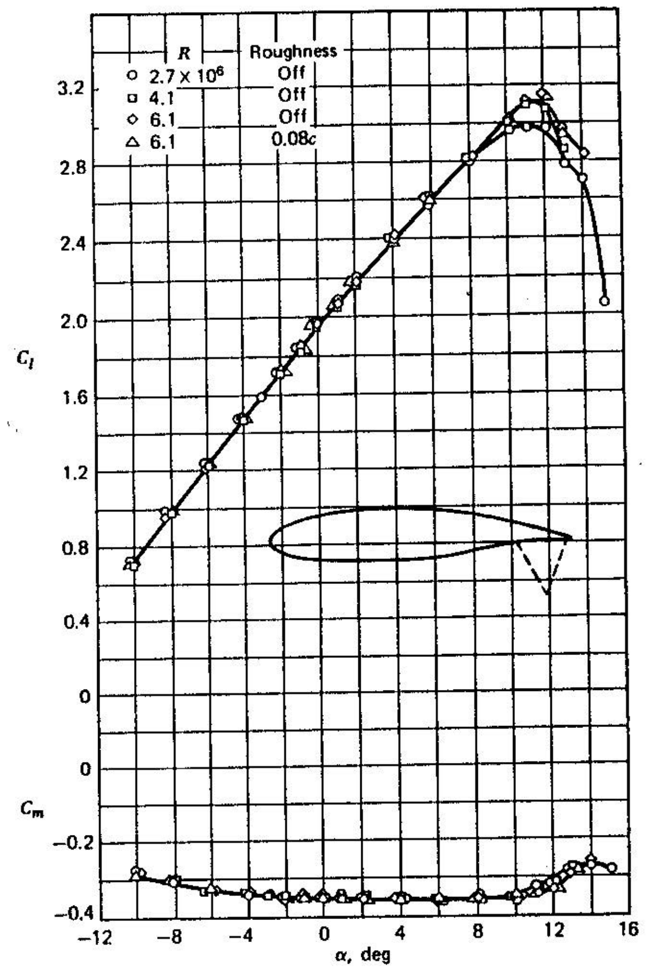

Figure 3.10c GA(W)-1 airfoil section characteristics for 0.20c simulated split flap

9

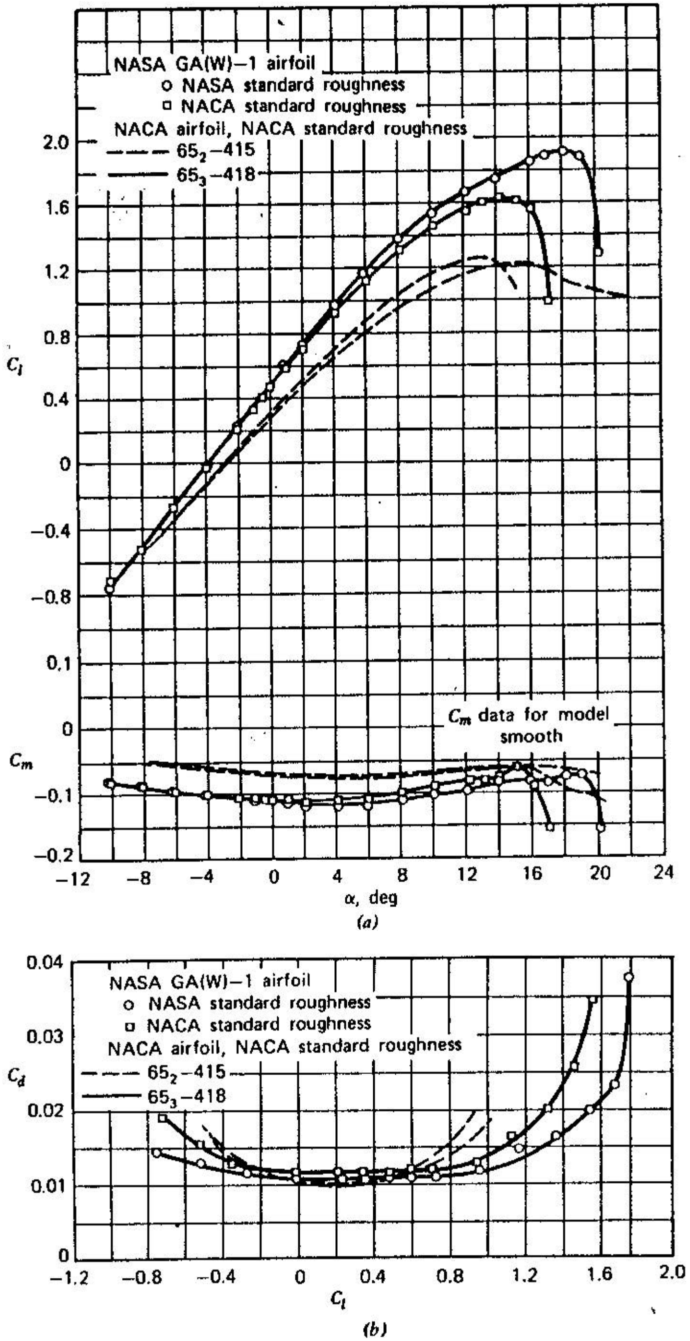

Figure 3.11 Comparison of section characteristics of NASA GA(W)-1 airfoil and NACA 65_2–415 and 65_3–418 airfoils. $M = 0.20$; $R \approx 6 \times 10^6$. (a) Variation of C_l and C_m

airfoils pictured in Figure 3.7. Test results for this airfoil are reported in Reference 3.8, where its $C_{l_{max}}$ values are shown to be about 30% higher than those for the older NACA 65-series airfoils. In addition, above C_l values of around 0.6, its drag is lower than the older laminar flow series with standard roughness. These data are presented in Figure 3.10 for the GA(W)-1 airfoil. Comparisons of $C_{l_{max}}$ and C_d for this airfoil with similar coefficients for other airfoils are presented in Figures 3.11 and 3.12.

Observe that the performance of the GA(W)-1 airfoil is very Reynolds number-dependent, particularly $C_{l_{max}}$, which increases rapidly with Reynolds number from 2 to 6 million. At the time of this writing, the GA(W) airfoil is beginning to be employed on production aircraft. The same is true of the supercritical airfoil. Indeed, the supercritical airfoil is being used on both the Boeing YC-14 and McDonnell-Douglas YC-15 prototypes currently being tested for the advanced medium STOL transport (AMST) competition. At the time of this writing, NASA is adopting a new nomenclature for the GA(W) airfoils. They will be designated by LS (low speed) or MS (medium speed) followed by four digits. For example, the GA(W)-1 airfoil becomes LS(1)-0417. The (1) designates a family. The 04 refers to a design lift coefficient of 0.4, and 17 is the maximum

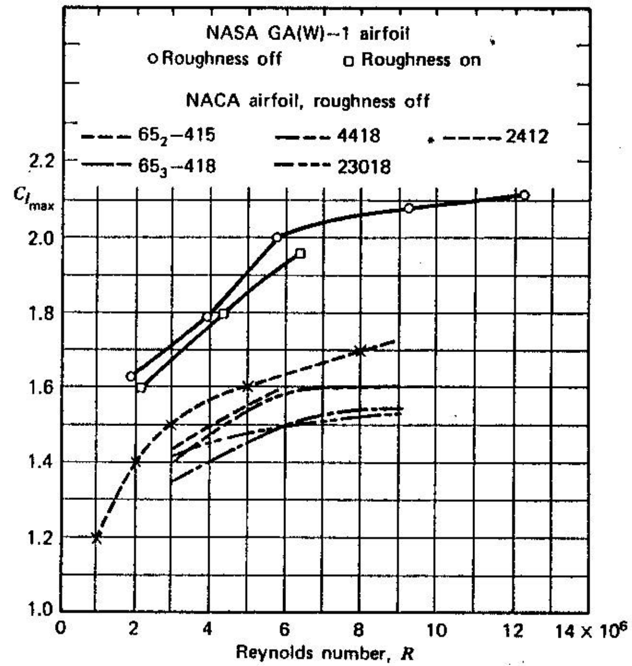

Figure 3.12 Comparison of maximum lift coefficient of the GA(W)-1 airfoil with other NACA airfoils $M = 0.15$.

10

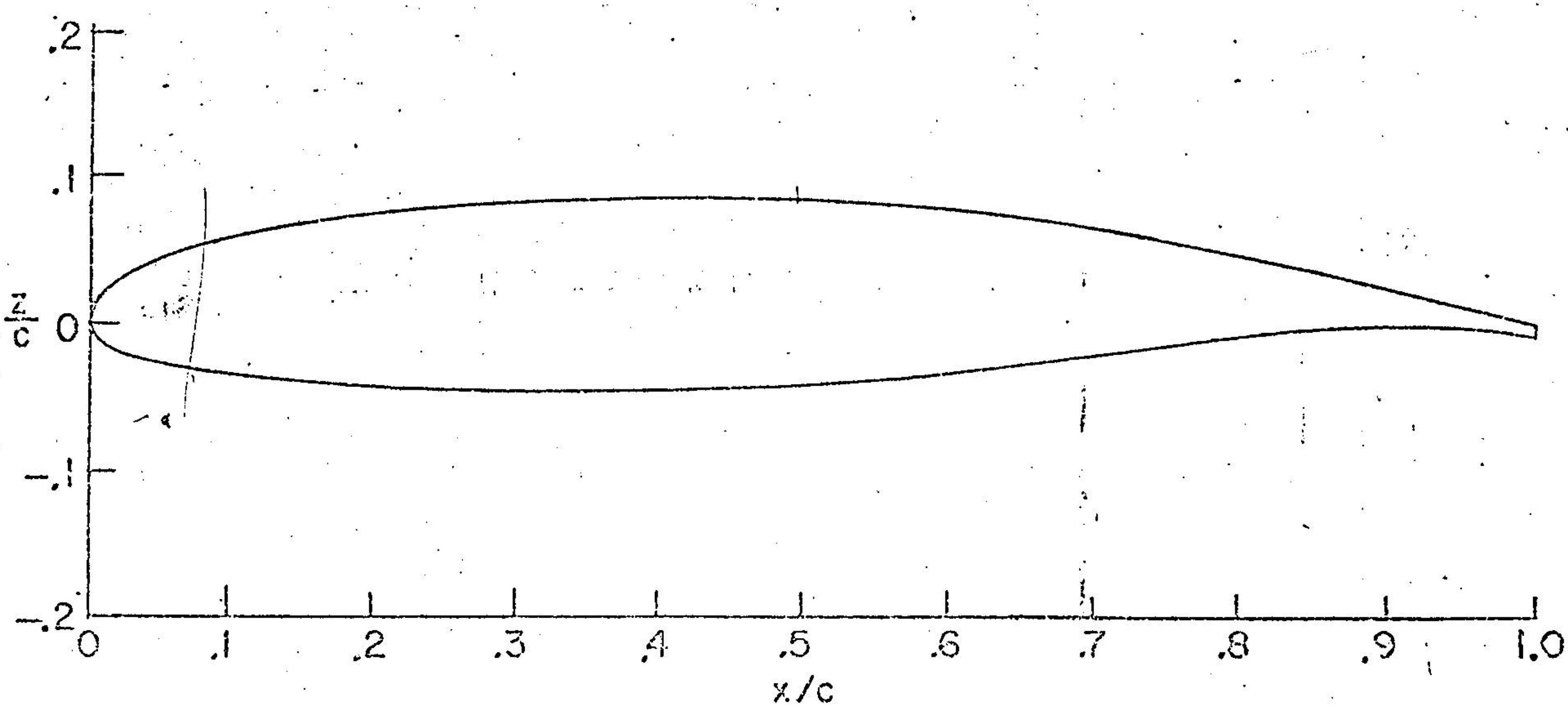

Figure 1. - Section shape for NASA GA(W)-2 airfoil.

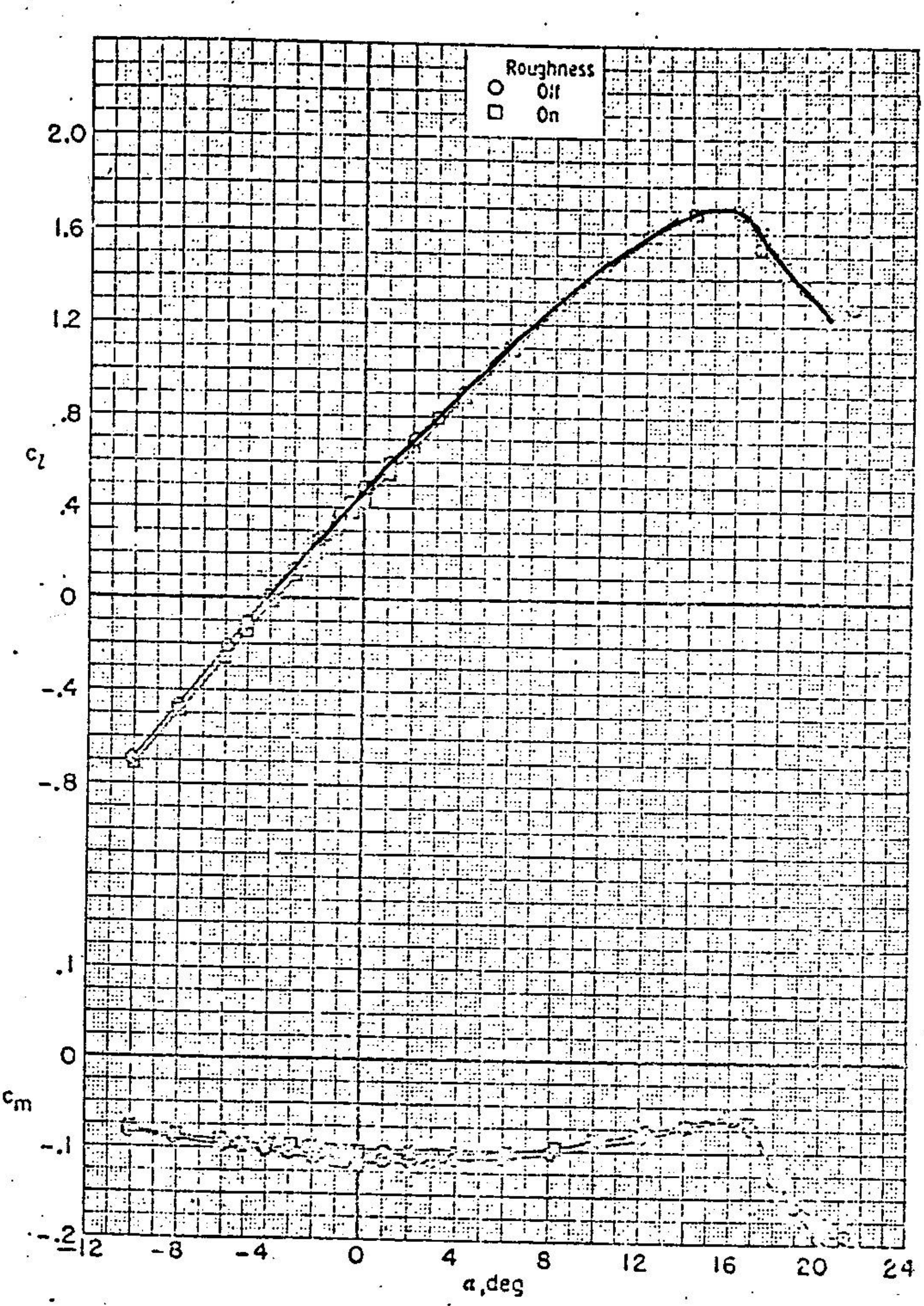

(a) $R = 2.1 \times 10^6$.

Figure 6. - Effect of Reynolds number on airfoil section characteristics. $M = 0.15$.

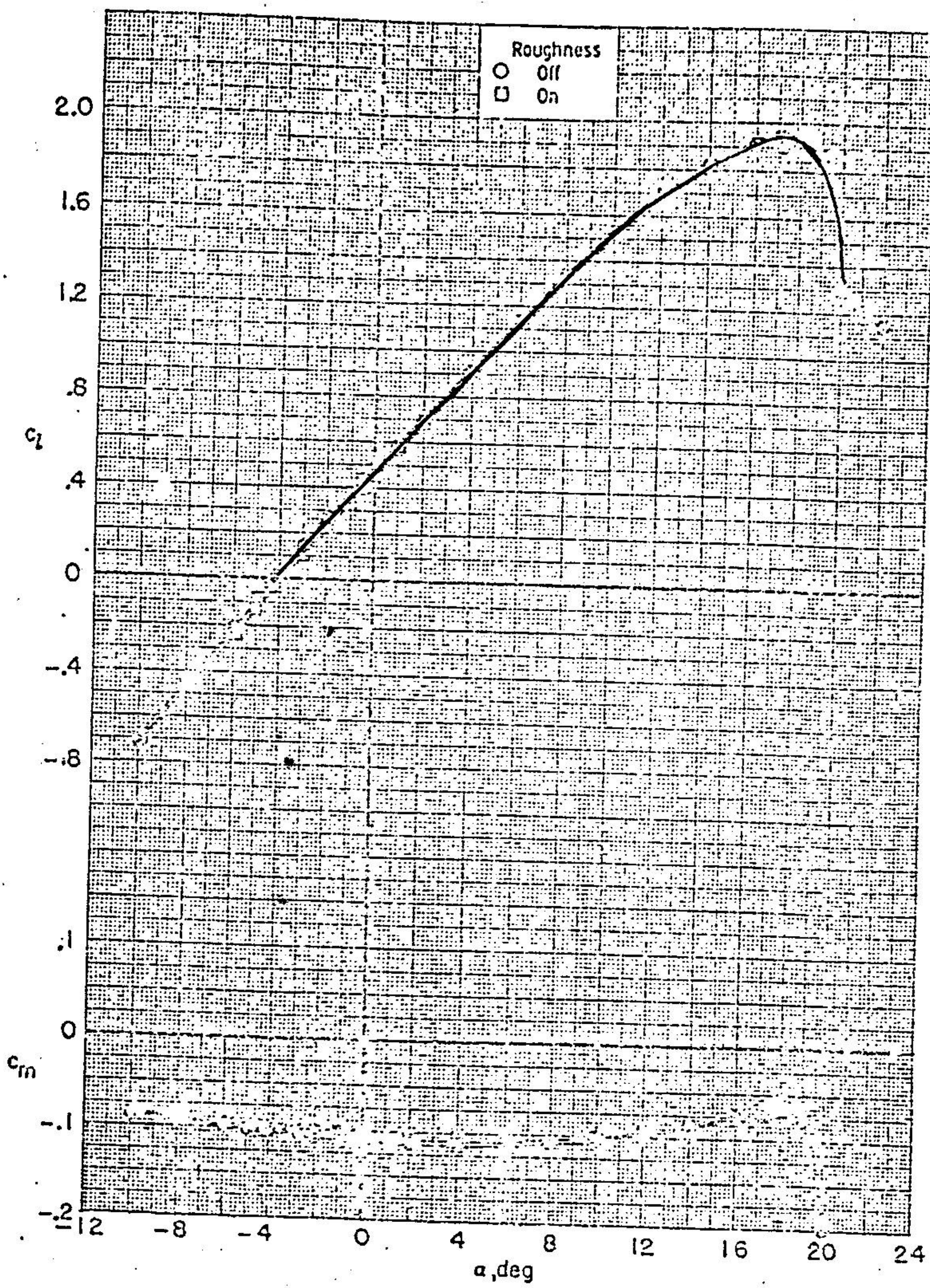

(c) $R = 4.1 \times 10^6$.

Figure 6. - Continued.

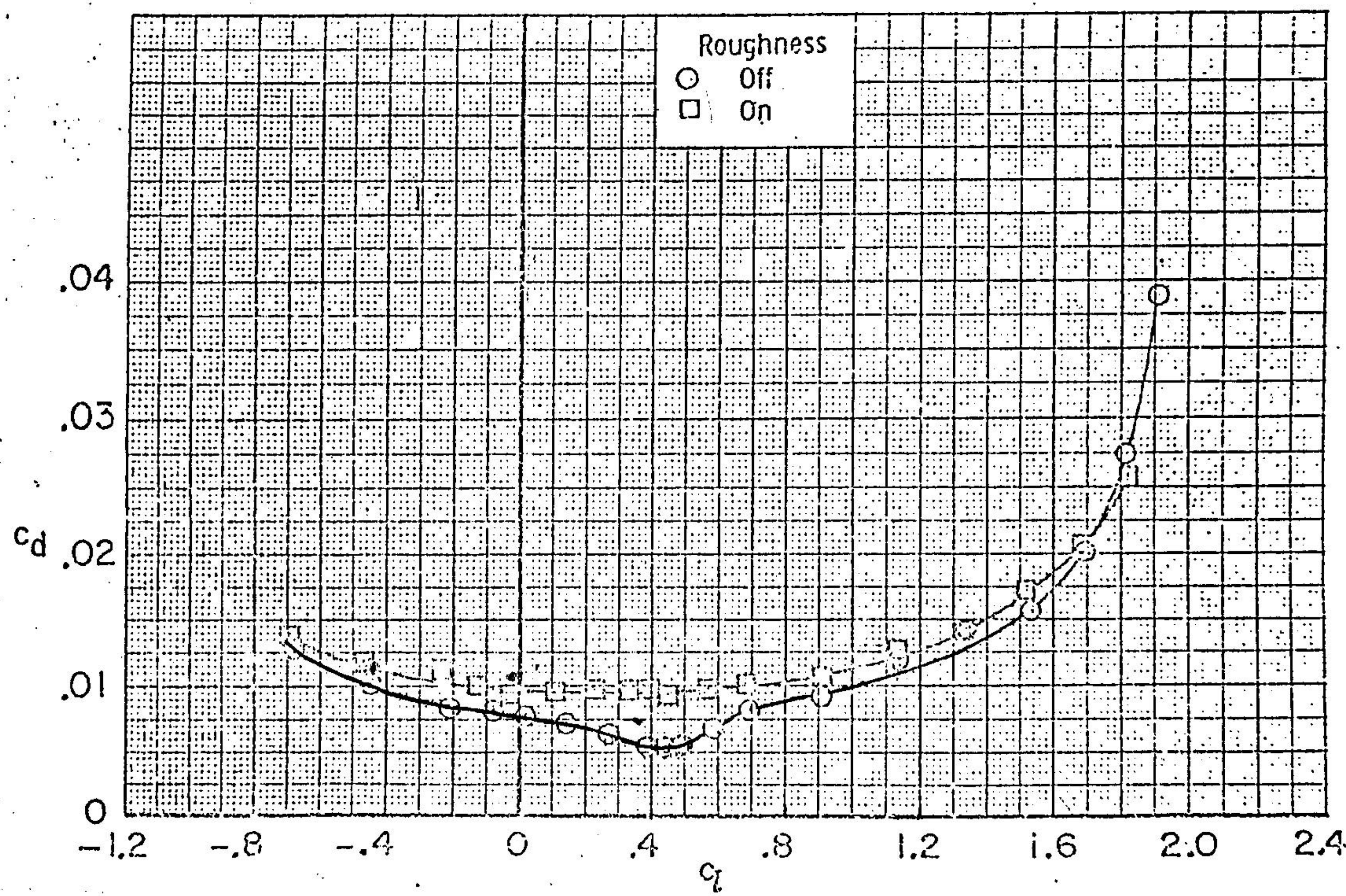

(c) $R = 4.1 \times 10^6$. Concluded.

Figure 6. - Continued.

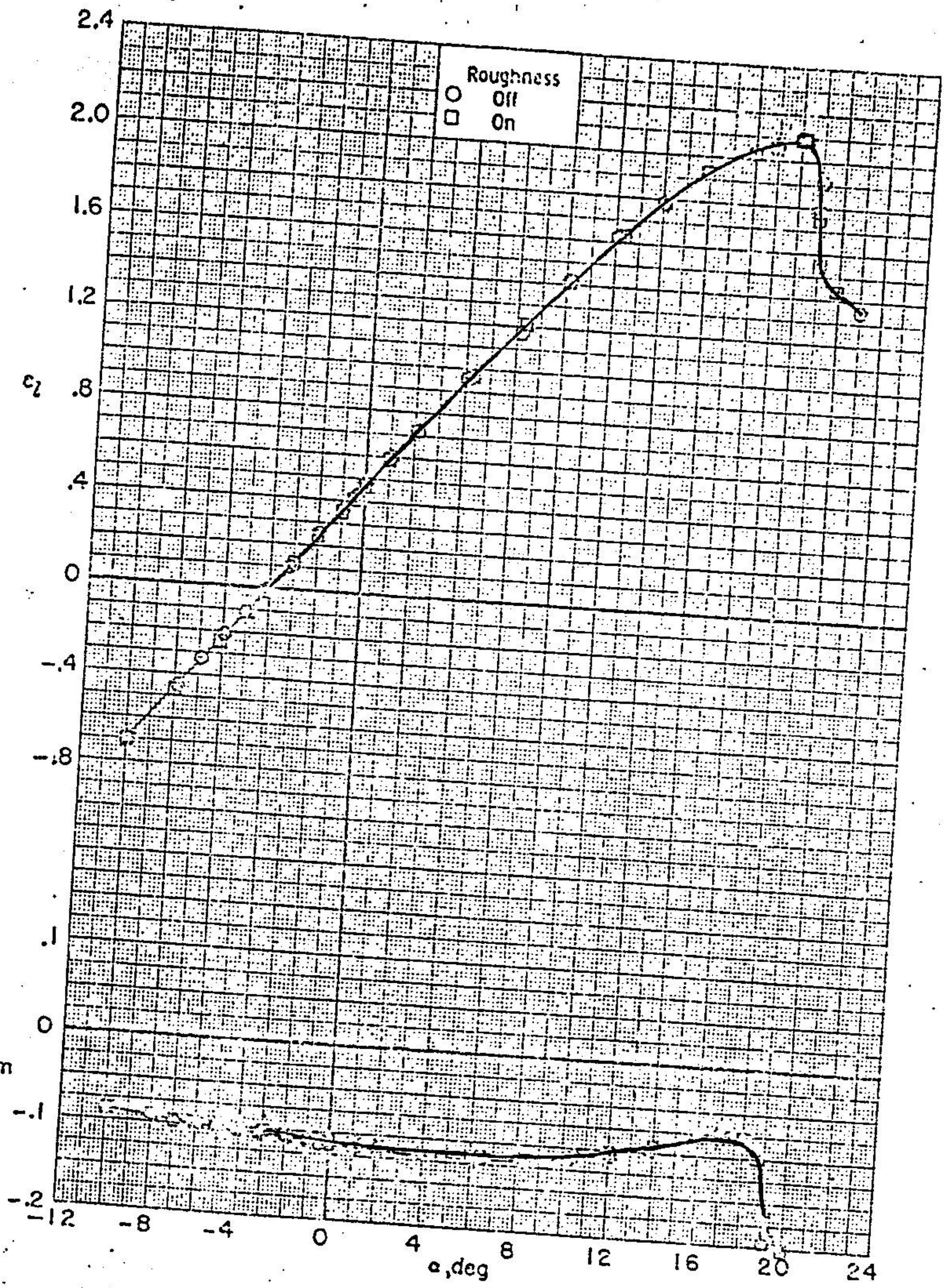

(e) $R = 9.4 \times 10^6$.

Figure 6. - Continued.

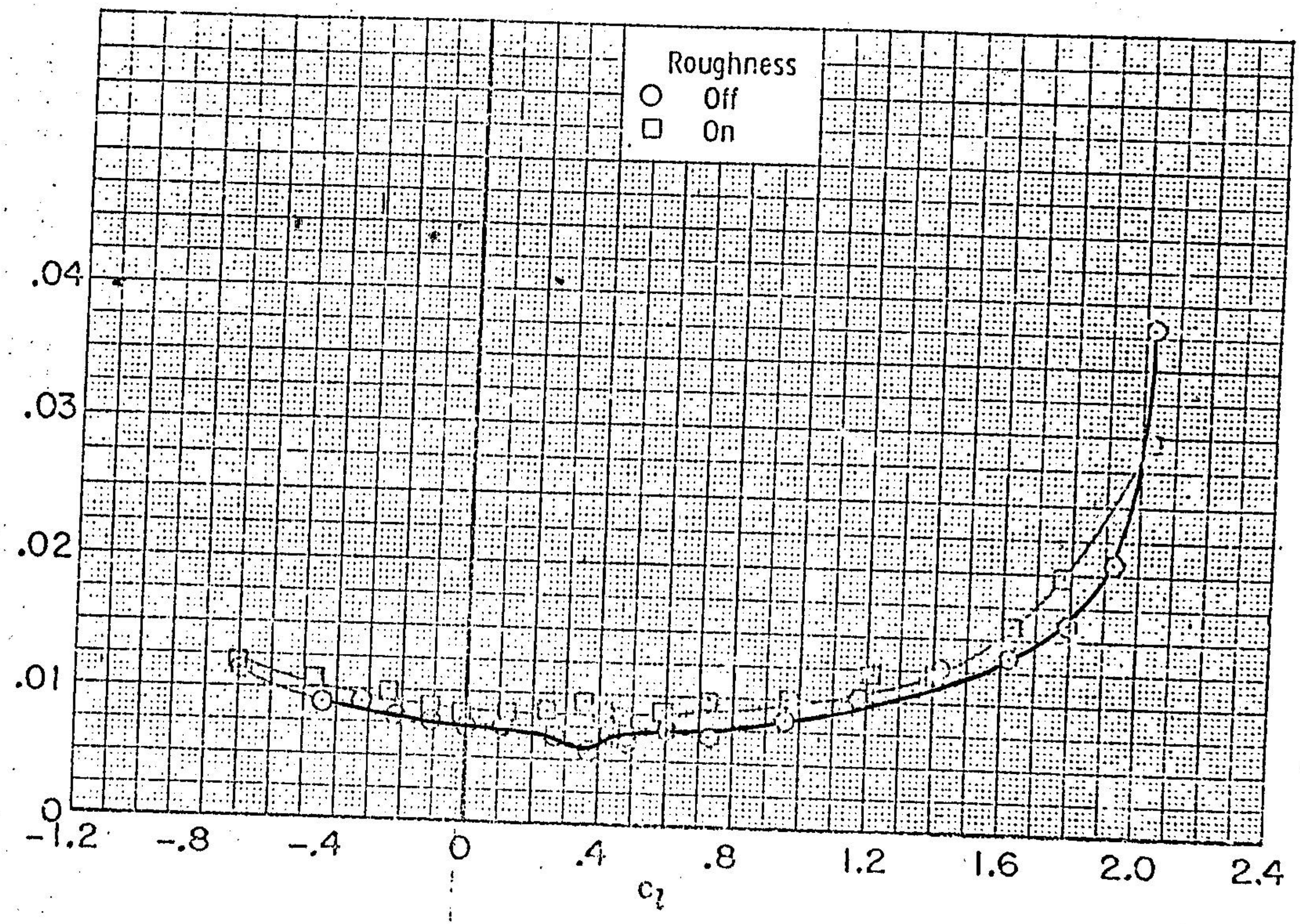

(e) $R = 9.4 \times 10^6$. Concluded.

Figure 6.-- Concluded.

NOTE: FOR SUPERCRITICAL AIRFOILS USE $\Delta M_{CR} = 0.05$

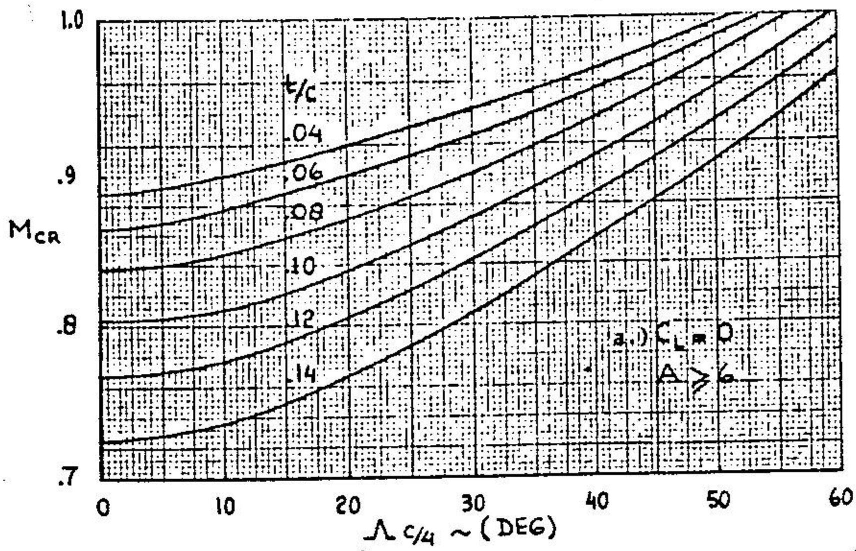

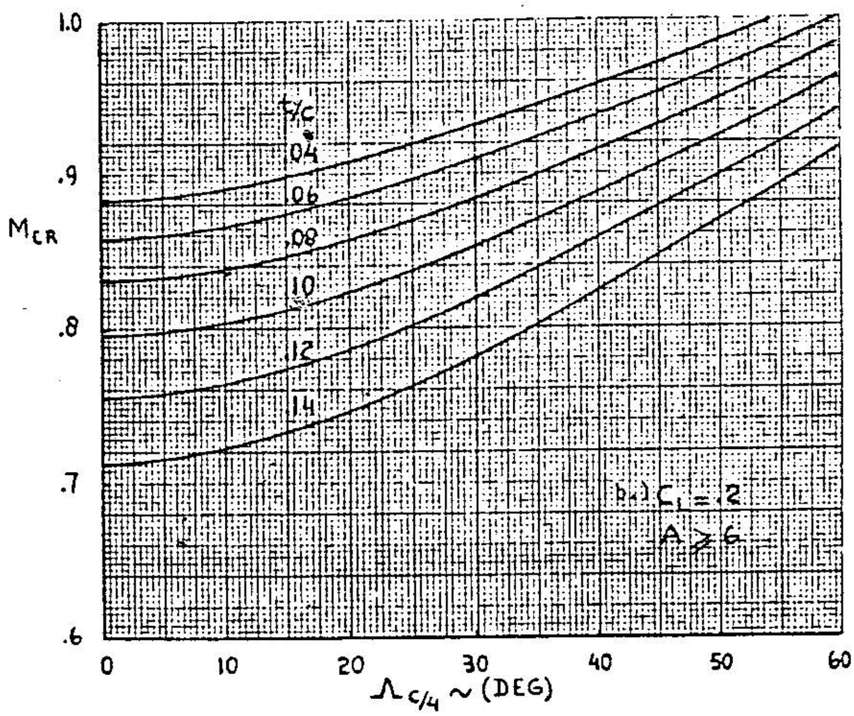

Figura 6.1a *Effetto del massimo spessore percentuale e dell'angolo di freccia sul numero critico di Mach*

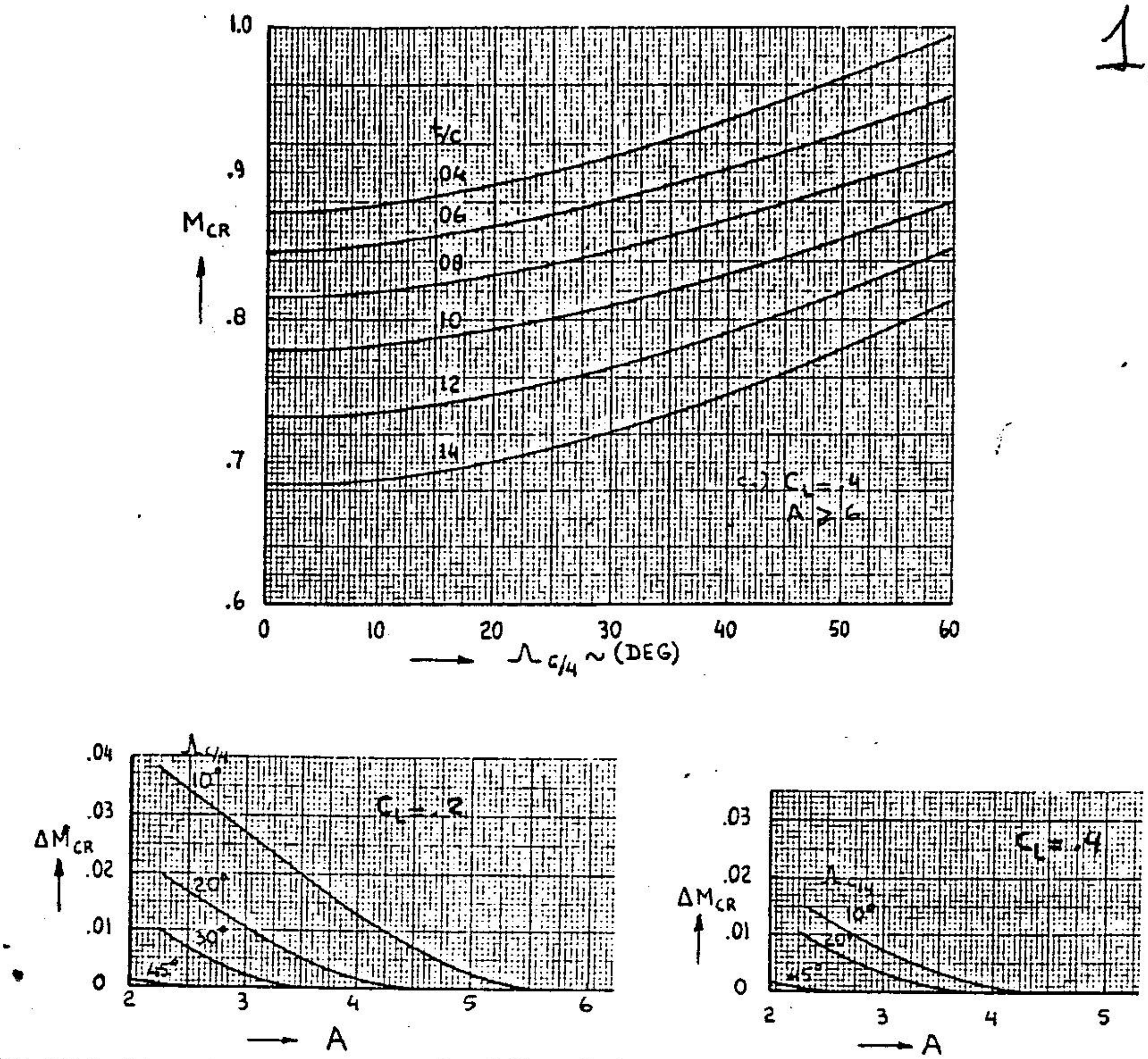

Figura 6.1b *Effetto del massimo spessore percentuale e dell'angolo di freccia sul numero critico di Mach*

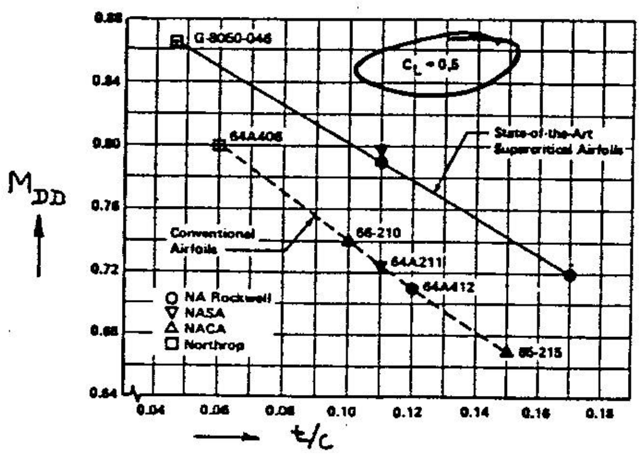

VERY ROUGHLY:

$M_{DD} = M_{CR} + 0.1$

Figura 6.2 *Effetto del massimo spessore percentuale sul numero di Mach di divergenza per alcuni profili NACA e supercritici*

Of greater practical interest is the so–called drag divergence Mach number, M_{dd}. This was also defined in Chapter 3 for an airfoil. Two definitions were given: the Boeing and Douglas definition respectively. These definitions are repeated next, as applied to the entire airplane.

a) Boeing Definition

M_{dd} is that free stream Mach number for which the drag due to compressibility first reaches 20 drag counts ($\Delta C_D = 0.0020$) above the incompressible level.

b) Douglas Definition

M_{dd} is that free stream Mach number for which the slope of the dragrise, $\delta C_D/\delta M$, first reaches the value 0.10.

These definitions are most easily applied when the drag rise behavior of airplanes is represented in a cross–plot of drag coefficient, at constant lift coefficient, versus Mach number. The reader is asked to apply these definitions to the dragrise behavior at different lift coefficients of the B–727–100 and the S–211 of Figure 5.3 and determine how closely they agree.

According to Chapter 4 (Figure 4.22), both critical Mach number and drag divergence Mach number depend strongly on the sweep angle. As it turns out, they also depend on the thickness ratio of lifting surfaces. These effects are illustrated in Figure 5.4 for conventional, non–super–critical airfoils.

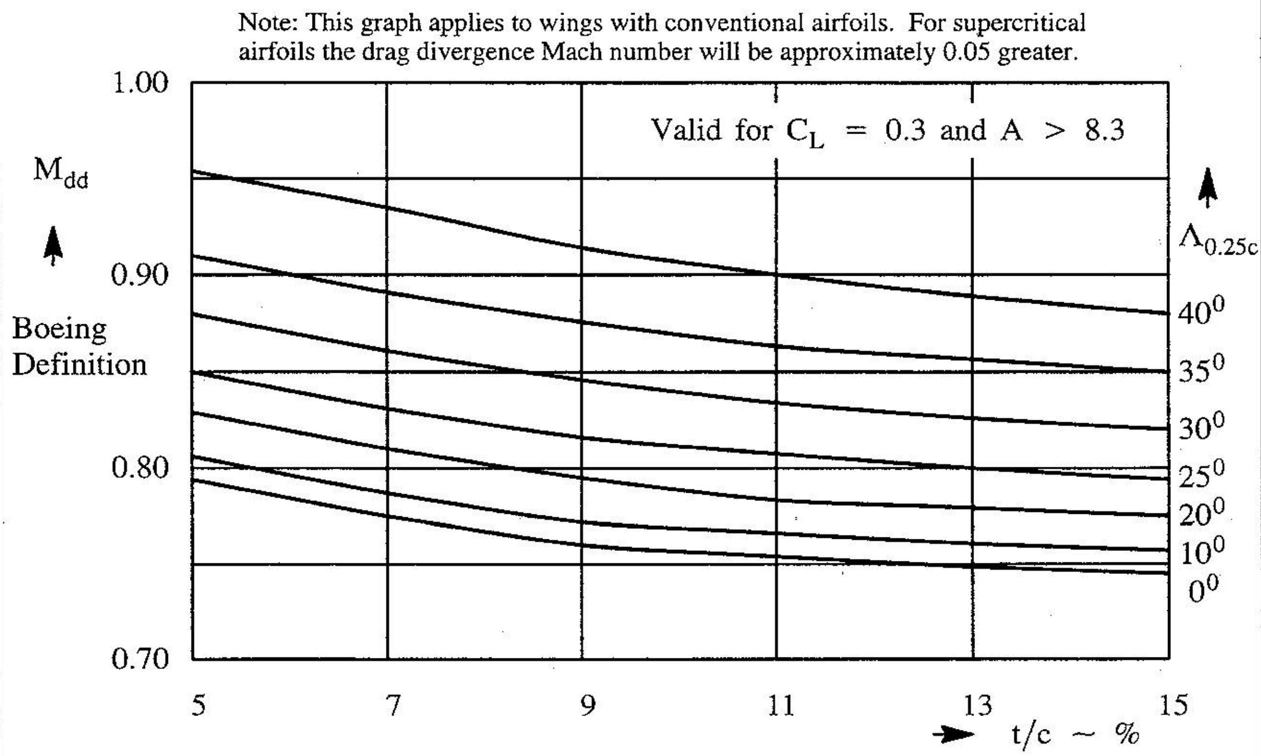

Figure 5.4 Effect of Wing Sweep and Thickness Ratio on Drag Divergence Mach Number

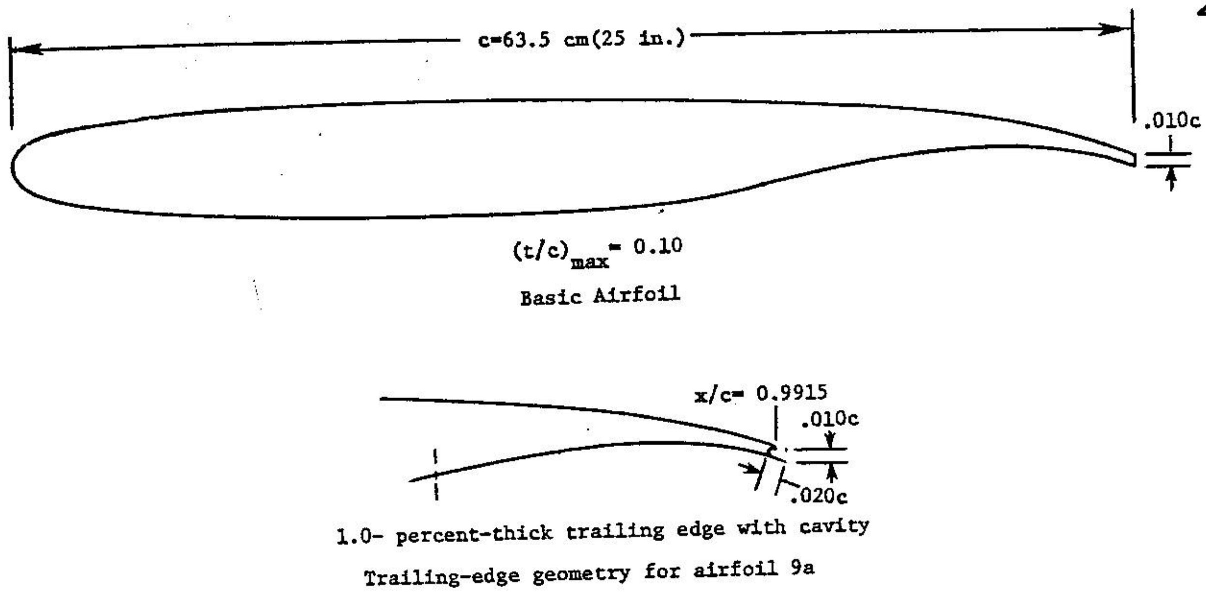

Figure 9.1.- Airfoil Geometry

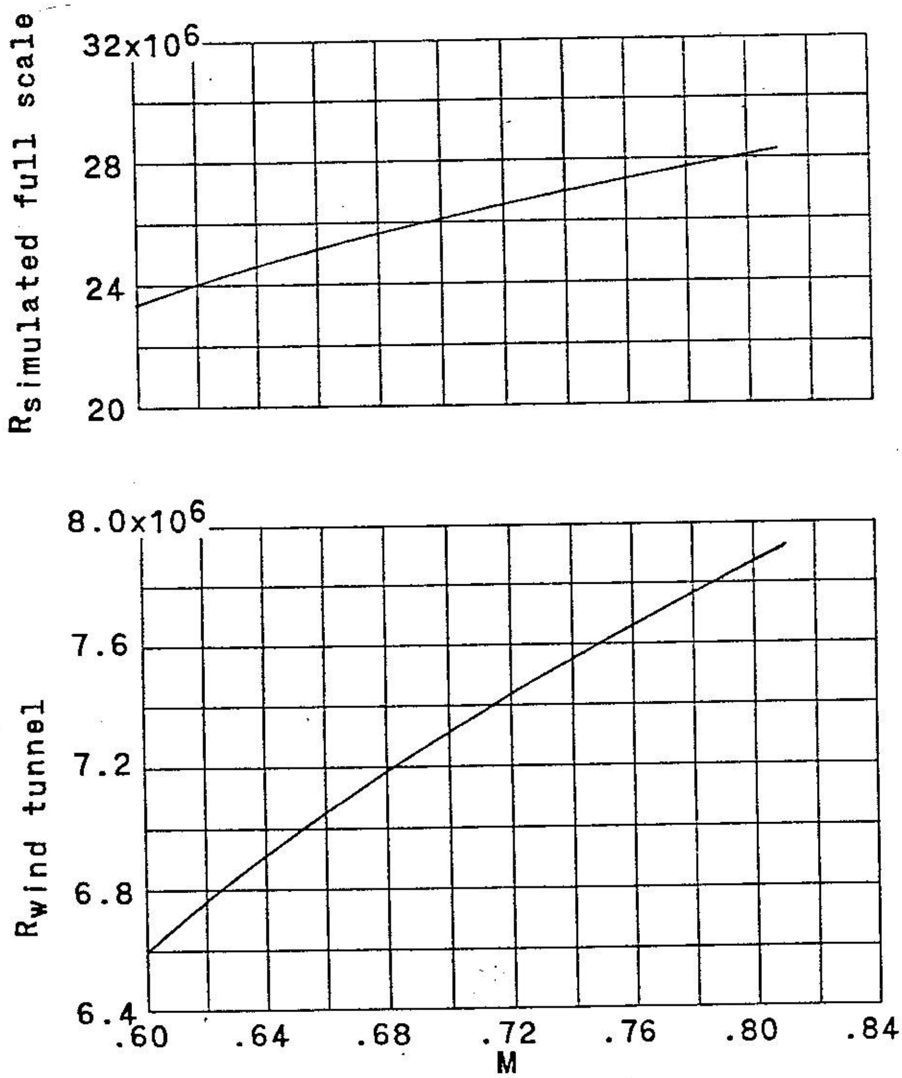

Figure 9.2.- Variation with Mach number of test wind-tunnel Reynolds number and simulated full-scale Reynolds number.

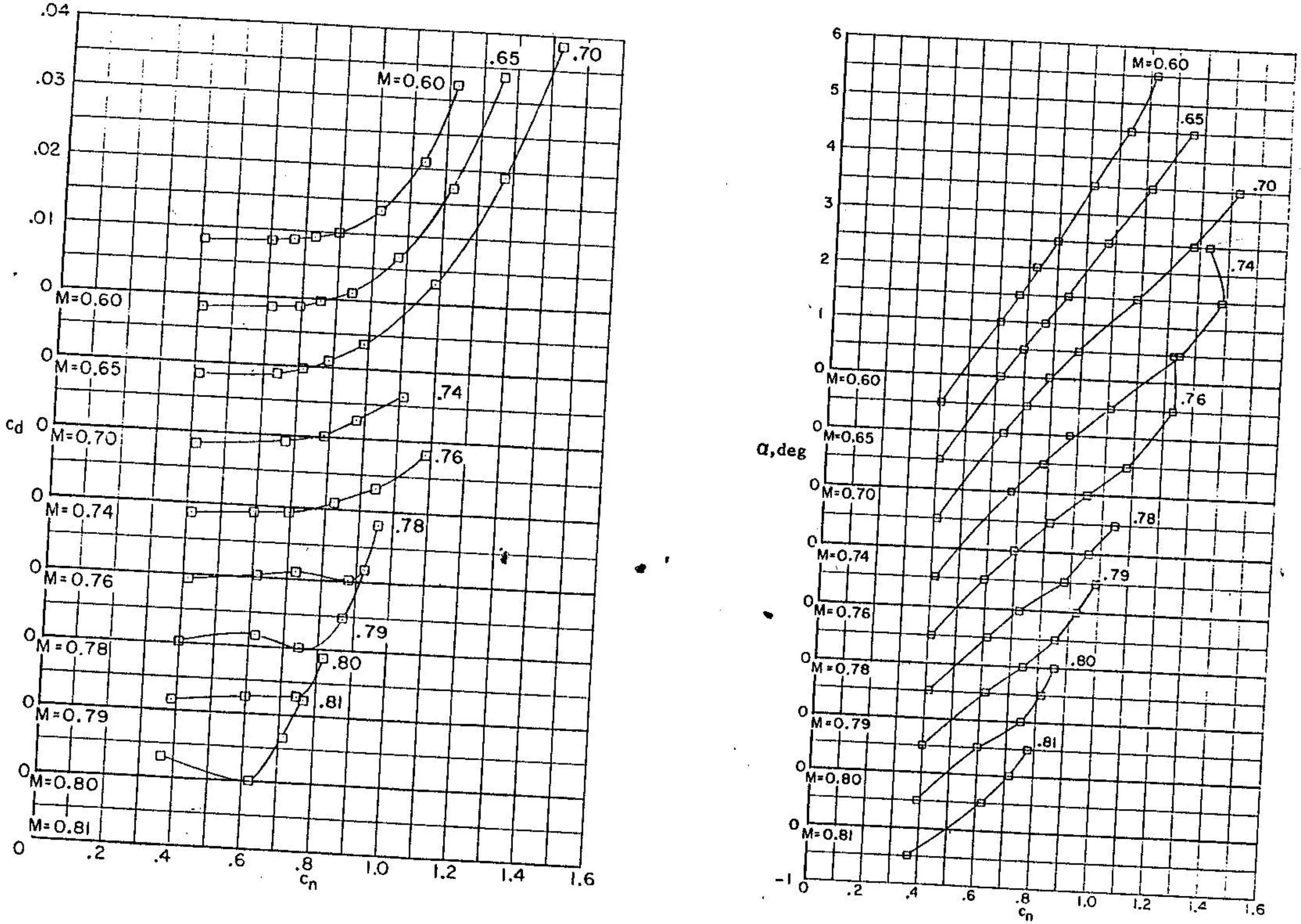

Figure 9.5.- Variation of section drag coefficient, angle of attack, and section pitching-moment coefficient at various Mach numbers.

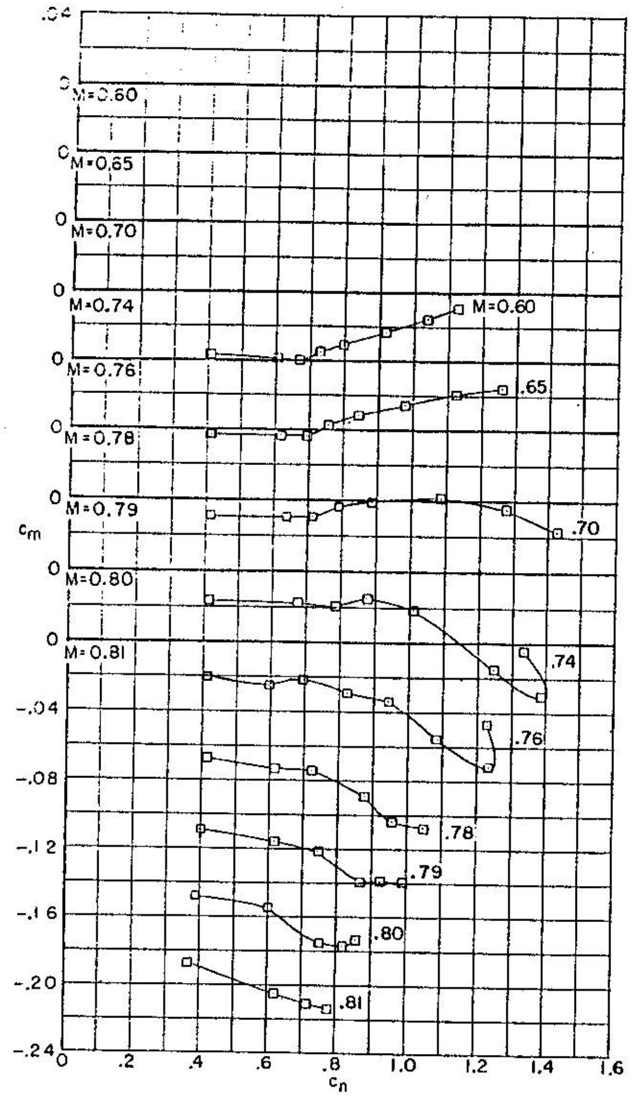

Figure 9.5.- Concluded.

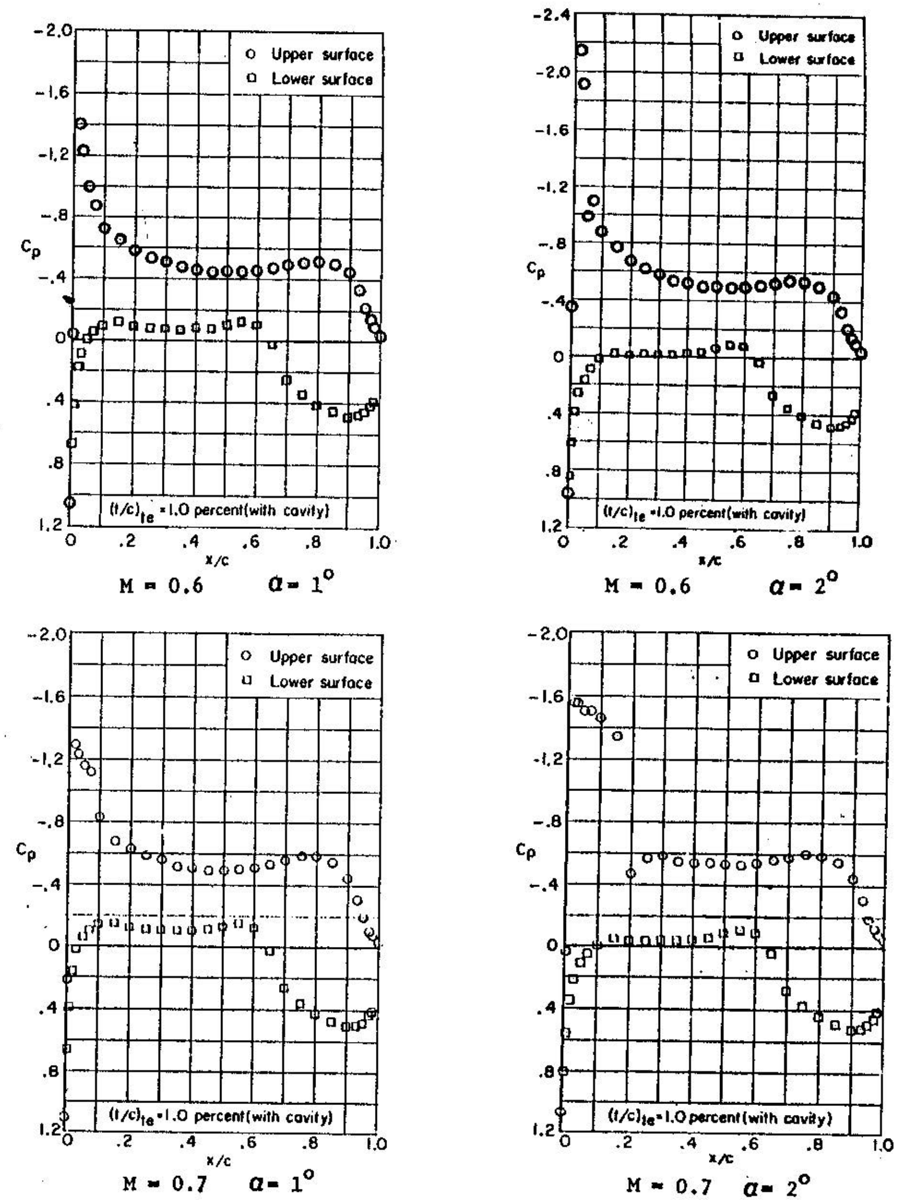

Figure 9.6.- Chordwise pressure distributions for various Mach numbers and angles of attack.

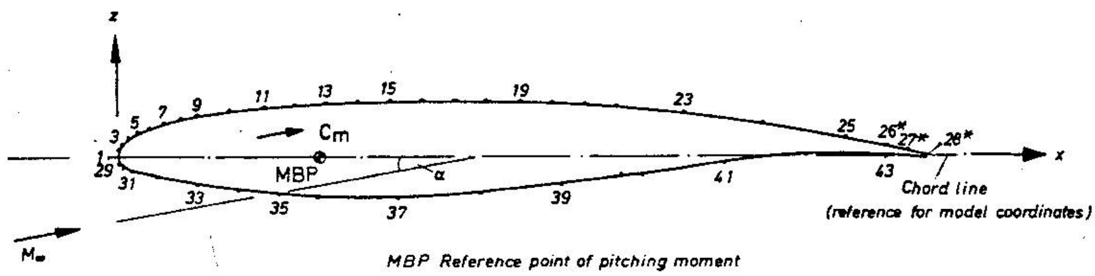

Geometric data: Chord c = 200 mm Maximum t/c = 11.8 % at x/c = 35 % Cross section $F_p \approx 3063 mm^2$
Trailing edge thickness z_{TE}/c = 0.38 % Diameter of pressure orifices d_B = 0.5 mm

a. Contour and location of pressure orifices

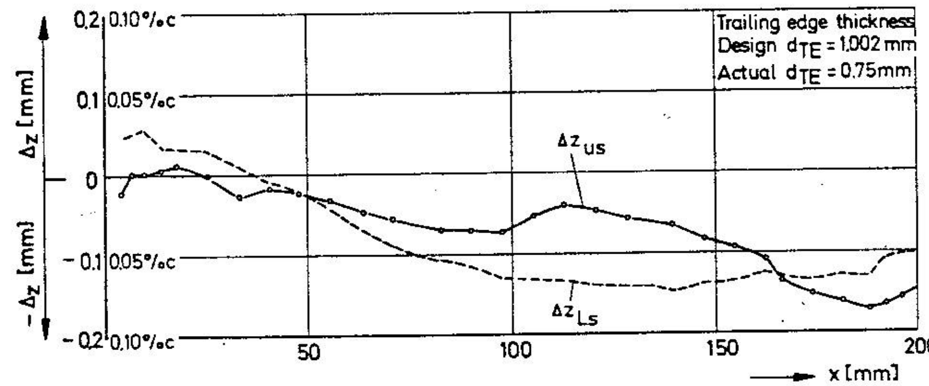

b. Measured error of manufactured airfoil (also see Table 3.1a)

Figure 3.1 Airfoil CAST 7 - Model SP 120 (c = 200 mm): Contour, location of pressure orifices and deviation from design coordinates (see Table 3.1b for deviation on ARA model)

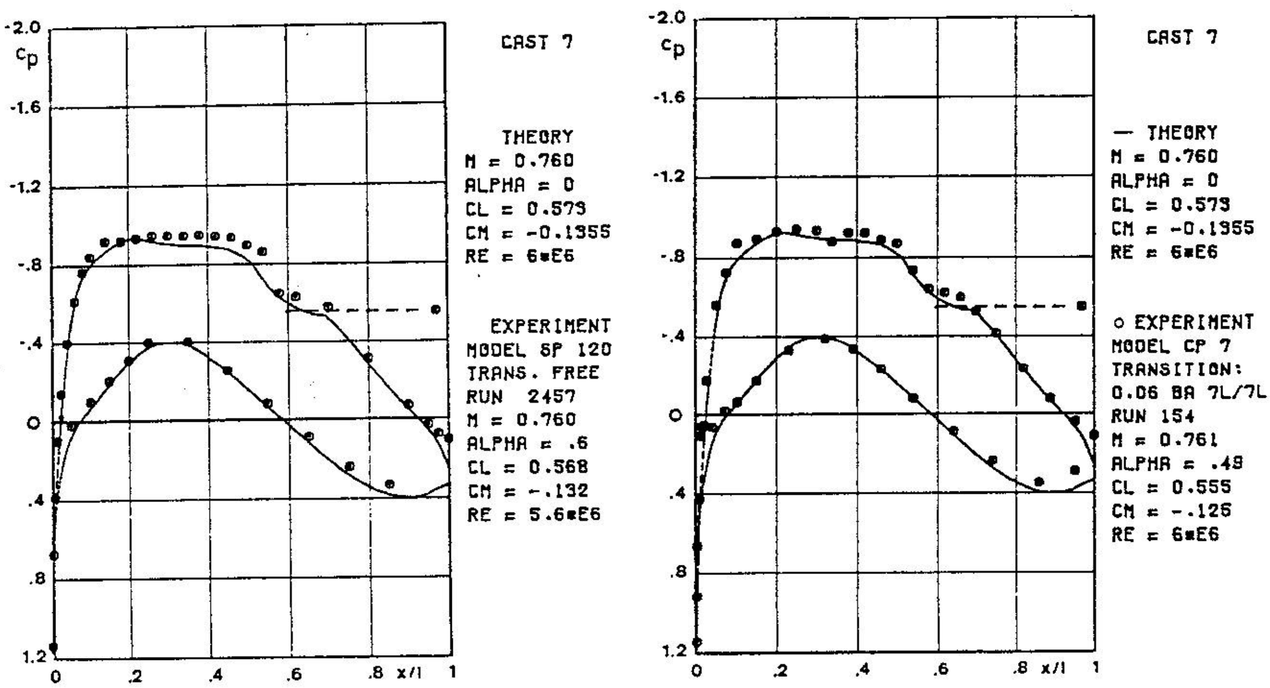

a. DFVLR - TWB tests

b. ARA tests

Figure 3.2 Design pressure distribution. Comparison between theory and experiment.